frontiers in Energy Research

ORIGINAL RESEARCH
published: 26 November 2020
doi: 10.3389/fenrg.2020.595224

Techno-Economic Assessment of Demand-Driven Small-Scale Green Hydrogen Production for Low Carbon Agriculture in Sweden

Leandro Janke[1], Shane McDonagh[2], Sören Weinrich[3], Daniel Nilsson[1], Per-Anders Hansson[1] and Åke Nordberg[1]*

[1]*Department of Energy and Technology, Swedish University of Agricultural Sciences, Uppsala, Sweden,* [2]*MaREI Centre, Environmental Research Institute, University College Cork, Ireland,* [3]*Department of Biochemical Conversion, Deutsches Biomasseforschungszentrum gemeinnützige GmbH, Leipzig, Germany*

Wind power coupled to hydrogen (H_2) production is an interesting strategy to reduce power curtailment and to provide clean fuel for decarbonizing agricultural activities. However, such implementation is challenging for several reasons, including uncertainties in wind power availability, seasonalities in agricultural fuel demand, capital-intensive gas storage systems, and high specific investment costs of small-scale electrolysers. To investigate whether on-site H_2 production could be a feasible alternative to conventional diesel farming, a model was built for dynamic simulations of H_2 production from wind power driven by the fuel demand of a cereal farm located on the island of Gotland, Sweden. Different cases and technological scenarios were considered to assess the effects of future developments, H_2 end-use, as well as production scale on the levelised- and farmers' equivalent annual costs. In a single-farm application, H_2 production costs varied between 21.20–14.82 €/kg. By sharing a power-to-H_2 facility among four different farms of 300-ha each, the specific investment costs could be significantly decreased, resulting in 28% lower H_2 production costs than when facilities are not shared. By including delivery vans as additional H_2 consumers in each farm, costs of H_2 production decreased by 35% due to the higher production scale and more distributed demand. However, in all cases and technological scenarios assessed, projected diesel price in retailers was cheaper than H_2. Nevertheless, revenues from leasing the land to wind power developers could make H_2 a more attractive option even in single-farm applications as early as 2020. Without such revenues, H_2 is more competitive than diesel where power-to-H_2 plants are shared by at least two farms, if technological developments predicted for 2030 come true. Also, out of 20 different cases assessed, nine of them showed a carbon abatement cost lower than the current carbon tax in Sweden of 110 €/tCO_2, which demonstrate the potential of power-to-H_2 as an effective strategy to decarbonize agricultural systems.

Keywords: green hydrogen, modeling and simulation, process optimization, techno-economic assessment, CO_2 emission reduction

Edited by:
Benedetto Nastasi,
Sapienza University of Rome, Italy

Reviewed by:
Manuel Bailera,
University of Zaragoza, Spain
Qingchun Yang,
Hefei University of Technology, China

****Correspondence:***
Leandro Janke
leandro.janke@slu.se

Specialty section:
This article was submitted to Sustainable Energy Systems and Policies, a section of the journal Frontiers in Energy Research

Received: *15 August 2020*
Accepted: *20 October 2020*
Published: *26 November 2020*

Citation:
Janke L, McDonagh S, Weinrich S, Nilsson D, Hansson P-A and Nordberg Å (2020) Techno-Economic Assessment of Demand-Driven Small-Scale Green Hydrogen Production for Low Carbon Agriculture in Sweden. Front. Energy Res. 8:595224. doi: 10.3389/fenrg.2020.595224

INTRODUCTION

Renewable energy sources can be exploited in remote areas with limited interconnection such as islands and/or agricultural farmlands to increase energy independence and security. Recently, declining costs of solar and wind power combined with policies and incentives to tackle climate change have created favorable conditions to further expand renewable energy production in such regions. However, due to its intermittency and uncertainty (especially for wind), high levels of variable renewable energy (VRE) are challenging to integrate into current energy systems, frequently resulting in a mismatch between supply and demand. Such imbalances cause fluctuations in grid voltage and frequency, as well as curtailment of power production, considerably increasing the overall costs of the system.

For this reason, different energy storage technologies have been developed for several applications, in particular to avoid curtailment of power production, and to support stable operations of electric grids (Fischer et al., 2018b; Koohi-Fayegh and Rosen, 2020). To compensate for production fluctuations as well as providing benefits at the system level (e.g., control reserve energy), H_2 based storage systems have been proposed (Grueger et al., 2017). Also, as a clean and versatile energy carrier, H_2 may have an important role in future low-carbon pathways, for instance, to produce gaseous (e.g., CH_4 and NH_3) and liquid fuels (e.g., methanol, gasoline, and dimethyl ether), heat or even directly used as fuel for mobility (Hanley et al., 2018).

In grain-based agricultural systems, nitrogen fertilizers and fossil fuel consumption are responsible for the majority of the GHG emissions (Yan et al., 2015). Where VRE is deployed on farmland, an interesting concept to decarbonize agricultural activities is to also include H_2 storage. Thus, curtailment could be avoided and local renewable electricity could be used to produce H_2 to displace diesel as a fuel in tractors and/or used to make NH_3 for fertilizer via the Haber-Bosch process (Moreda et al., 2016; Allman and Daoutidis, 2018). While the latter may be restricted to large farming operations (minimum megawatt-scale equipment), H_2 as fuel could potentially be used in small- and mid-size farms since it has been successfully implemented at the kilowatt-scale in industrial applications such as welding and brazing, material handling vehicles (e.g., forklifts and airport towing trucks) as well as for mobility (e.g., golf cart and long-range passenger cars) (Allman et al., 2017; Apostolou et al., 2019). Thanks to its higher energy density compared to lithium-ion batteries, H_2-based fuel cell agricultural machinery (FCAM) may be preferred to manned battery-electric since agricultural operations often require continuous hours of heavy fieldwork (NHA, 2012; Wu et al., 2019; Lagnelöv et al., 2020). In addition, during the conversion of electricity to H_2 via water electrolysis, oxygen (O_2) and low-temperature waste heat (WH) at 60–90°C are produced which could be valorized (Buttler and Spliethoff, 2018). For instance, WH could be used for drying grains or heating greenhouses, while O_2 could be used in aquaculture, in particular for sensitive species like salmon and trout (García et al., 1998; Mariani et al., 2016; Linde, 2017b). These applications should improve the sustainability of the concept as well as reduce costs associated with H_2 production.

However, the on-farm production of H_2 to be used in FCAM is challenging: 1) farming is a highly seasonal activity in which typical operations like harrowing, sowing, fertilizing, plowing and harvesting occur over short periods of time, resulting in peaks of fuel demand; 2) VRE production is uncertain by nature increasing risks of mismatch between supply and demand; 3) Large gas storage to compensate for such seasonalities are capital-intensive, and 4) decentralized small-scale electrolysers have higher specific investment costs increasing production costs compared to larger facilities.

Small-scale H_2 production via water electrolysis has been investigated for different applications. For instance, Fischer et al. (2018a) developed a predictive control model for a 120 kW proton exchange membrane (PEM) electrolyser, injecting H_2 into the natural gas grid according to fluctuating electricity prices in the spot market and within network limitations. In an energy system dominated by hydropower production, Ulleberg et al. (2020) examined the deployment of small-scale electrolysers coupled to H_2 refueling stations for fuel cell electric vehicles. Similarly, Apostolou et al. (2019) further down-scaled the process proposing the use of a 50 kW wind turbine coupled to a 70 kW alkaline electrolyser to supply H_2 for fuel cell electric bicycles in a green urban mobility concept. Also, H_2 refueling stations with electrolysers smaller than 500 kW to supply the demand of H_2 cars, and the optimization of an electrolyser operation employing wind, electricity prices, and H_2 demand have been investigated elsewhere (Grüger et al., 2018; Grüger et al., 2019). Furthermore, the feasibility of stationary power-to-gas systems to store excess electricity from renewable sources in buildings with different heat and power requirements have been assessed combined with oxy-fuel boilers to produce concentrated CO_2 stream and facilitate further methanation of H_2 (Bailera et al., 2018; Bailera et al., 2019). Even though previous studies addressed H_2 production from solar PV to fuel an all-wheel drive vehicle on a winery (Carroquino et al., 2018; Roda et al., 2018), to the best of the authors' knowledge, techno-economic assessments of on-farm H_2 production based on wind power to supply the fuel demand of heavier agricultural machineries like tractors and harvesters have never been reported. Such a concept could provide multiple benefits, curtailment could be avoided increasing the income of wind power project developers, locally produced clean fuel would be provided to decarbonize agricultural activities, and land leasing payments would be provided to farmers.

In Sweden, the local authorities of Gotland's island have committed to an ambitious plan to be self-sufficient in energy by 2025. For this reason, local wind power production is planned to increase 5-fold (to around 1,000 MW) while grid interconnection to the mainland will be restricted to 500 MW. Nowadays, major efforts are being made by different research initiatives to develop feasible options to store and manage excess electricity that may occur (GEAB, Vatenfall, ABB, and KTH, 2011; Byman, 2015; Mohseni et al., 2017; Wallnerström and Bertling Tjernberg, 2018). Our study differentiates from previous investigations by focusing on developing a modeling tool for discrete-event simulation of H_2 production according to the fuel demand of cereal-based farms located on Gotland. The model was used to find optimal plant configurations that minimized the levelized cost of H_2 ($LCOH_2$) according to the following cases: 1) single-farm H_2 production for FCAM; 2) shared infrastructure between two farms for FCAM and fuel cell minivan (FCMV); and 3) increased scale production by sharing the PtH_2 plant among four farms for FCAM and FCMV. Optimal plant configurations were used for further assessment of the equivalent annual cost (EAC) to compare the cost of ownership of FCAM and conventional diesel agricultural machinery in different technological scenarios (2020 and 2030). Additionally, to provide insights for policymakers on possible decarbonization strategies, the carbon abatement cost of each case assessed was also calculated.

METHODOLOGY

System Description

The power-to-hydrogen (PtH_2) plant refers to an electrolyser, compressor, storage system, and a dispenser located on a farm on the island of Gotland, Sweden (57°30′N 18°33′E/57°50′N 18°55′E). A proton-exchange membrane (PEM) electrolyser was chosen due to its suitability for small-scale applications. The overall reaction of H_2 production by water electrolysis is shown in **Eq. 1**:

$$H_2O\,(l) \rightarrow H_2\,(g) + \frac{1}{2}O_2\,(g) \quad \Delta H_R^0 = +286\ \text{kJ/mol} \tag{1}$$

The electricity is primarily obtained from wind turbines located inside the farm boundary. However, during system downtime and for safety infrastructure, electricity is also obtained from the grid (regulated market) in small volumes. To allow storage at 500 bar, H_2 is compressed as soon as it is produced in the stacks (Linde, 2014). The H_2 is supplied according to the demand of FCAM and where applicable FCMV used for delivery (see *Agricultural H_2 Demand*). Additionally, the economic benefits of utilizing low-temperature WH at 60°C in a greenhouse for growing tomatoes (see Appendix A), and O_2 for on-site fish farming are considered (Linde, 2017a; Linde, 2017b; Törnfet and Nypelius, 2020).

In this system, farmers cooperate with wind power project developers in a business model where farmland is leased to wind power production securing additional revenues to farmers and improving wind power output, in case H_2 is produced at times of constrained power grid. **Figure 1** and **Table 1** show the technical system boundary and an overview of the characteristics of PEM electrolyser considered in the present study.

Dynamics of the Power-to-Hydrogen Plant Operation

The H_2 demand of FCAM and FCMV and the H_2 level in the storage tank determine whether the electrolyser should enter in operation. Therefore, whenever H_2 storage is low and wind power production is sufficient to run the electrolyser on full-load, H_2 is produced until the storage tank is full. At times of no wind power production or full H_2 storage, the system is put directly on cold standby since the time required to ramp-up a PEM electrolyser is negligible (Buttler and Spliethoff, 2018). Thus, cold standby solely defines the non-operating hours (NOH) of the system. The energy consumed during NOH and by the safety infrastructure is purchased from the regulated market with a fixed tariff of 100 €/MWh as the quantities are too low to qualify for a cheaper tariff (e.g., day-ahead spot market). A schematic diagram of the dynamic PtH_2 plant operation is presented in **Figure 2** (additional information is provided in *Power-to-Hydrogen Model and Optimization Procedure*).

Cases Assessed

To assess the influence of H_2 demand on the economic performance of the agricultural PtH_2 plant, different cases were investigated under the current and future technological scenarios (2020 and 2030). A single-user PtH_2 plant was used as a reference in case 1, while the option of sharing the PtH_2 with more than one farm was investigated in Cases 2a and 3a. The influence of having FCMV for delivery in addition to the H_2 demand of FCAM was investigated in Cases 2b and 3b. In all cases, wind power per land area was calculated as an average value according to local conditions found in Sweden (approx. 6.5 MW/km^2) (Stadkraft, 2020). Thus, wind power capacity was used to determine land lease revenues and, combined with the specific wind power production (see *Wind Power Production*), it was also used for modeling wind power production/availability for PtH_2 applications. A summary of all cases assessed is found in **Table 2**.

Wind Power Production

Historical wind speed measurements were used to simulate wind power production. Hourly values for 2017 were obtained from the meteorological station at the Visby Airport (57°66′N 18°34′E) on Gotland, Sweden. The station is located at 42 m above sea level and measures wind at 10 m high from the ground (SMHI, 2017). The wind speed and wind direction are shown as a wind rose in **Figure 3A** as well as the wind speed frequency (**Figure 3B**). Wind speed was extrapolated to the turbine hub height of 95 m using the power law with an exponent of 0.13 (McDonagh et al., 2020). The power curve of the V90 2.0 MW wind turbine (Vestas, Denmark) was used to convert wind speed into power for parks with 10–40 wind turbines depending on the case assessed (see *Agricultural H_2 Demand*). Such turbine cuts in at 4 m/s, is rated at 13 m/s, and cuts out at 25 m/s (Vestas, 2019).

Price of Electricity Used for H_2 Production

Hourly values from the day-ahead spot market of the Nord Pool power exchange were used to calculate the electricity costs to run the PtH_2 plant (NordPool, 2019). Thus, the electricity used is accounted for as an opportunity cost if the wind power operator would have the option to sell electricity to the grid. Even though electricity prices can vary significantly when different years are compared (Janke et al., 2020), 2017 was chosen since the average price found in this year is representative of historical values between 2013–2018 in Sweden. The price distribution in the day-ahead market of the Nord Pool power exchange for the SE3 region in 2017 is shown in **Figure 4**. We do not consider discounting the electricity price as the benefits offered to the

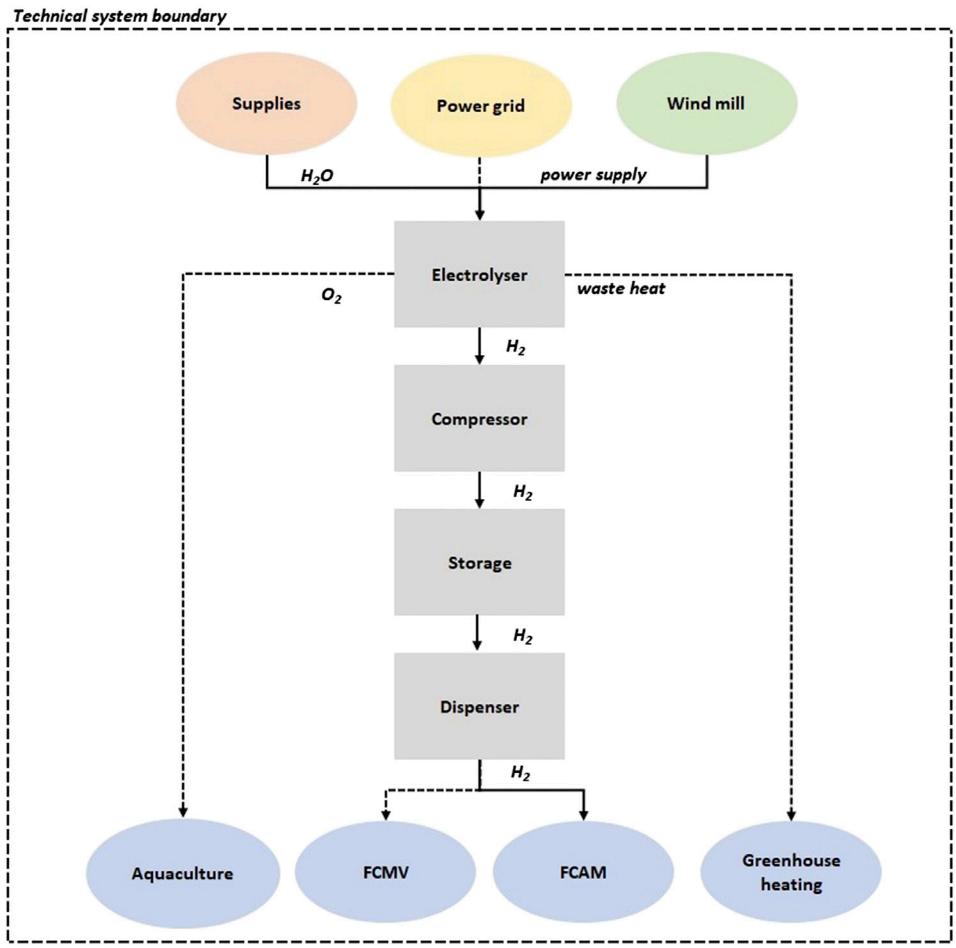

FIGURE 1 | Schematic diagram of the technical system boundary. Note: Dotted arrow lines represent optional H_2 and/or by-products use; FCMV - fuel cell minivan; FCAM - fuel cell agricultural machinery.

wind farm developer (reduced curtailment, system flexibility) are captured in the land leasing payment made to the landowner/farmer (see *Power-to-Hydrogen Model and Optimization Procedure*).

Agricultural H_2 Demand

In the present study, H_2 demand is modeled according to the requirements of two different consumers, namely FCAM (agricultural machinery) and FCMV (minivan). FCAM H_2 demand was estimated for a cereal farm in Sweden according to the model described by Lagnelöv et al. (2020) based on dynamic discrete-event simulation with embedded state-based logic for decision making. The simulated farm encompassed 300-ha equally distributed between barley, oats, spring wheat, and winter wheat crops. The model used a conventional cropping system with work beginning in mid-March and ending at the start

TABLE 1 | Specifications of the proton-exchange membrane (PEM) electrolyser.

Characteristics	Value		Source
	2020	2030	
Specific power consumption (kWh/m^3 H_2)	4.9	4.6	de Bucy et al., 2016; Schmidt et al., 2017; McDonagh et al., 2018
Conversion efficiency (%)	72.2	76.9	de Bucy et al., 2016; Schmidt et al., 2017; McDonagh et al., 2018
Cold start-up time (min)	5–10		Buttler and Spliethoff, 2018
Warm start-up time (sec)	10		Buttler and Spliethoff, 2018
Power input that becomes available heat (%)	17.1		Frank et al., 2018
Operation pressure (bar)	35		Proost, 2019

Note. Based on higher heating value (HHV) and standard temperature and pressure (STP) values (0°C and 101.325 kPa).

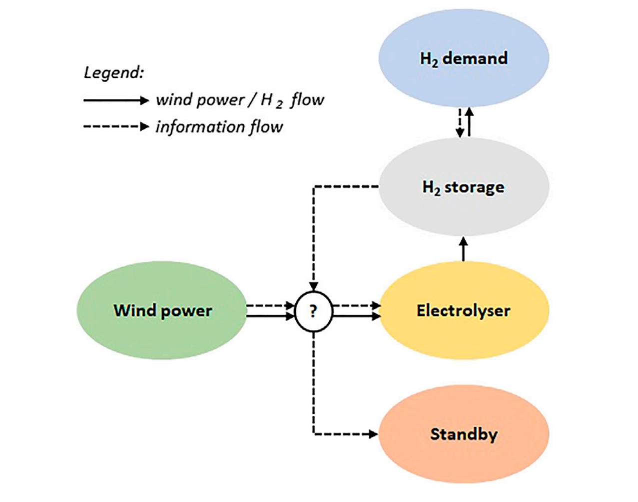

FIGURE 2 | Schematic diagram of the dynamic PtH_2 plant operation.

of November (Lagnelöv et al., 2020). One of the main aspects of this model is a workability control based on weather conditions and soil moisture content, which considered the water balance model described in (Witney, 1988) and tested by (Nilsson and Hansson, 2001). In the present study, weather and soil data from the island of Gotland (Sweden) were used instead of the values in the original report. The soil type on Gotland is mainly sand or sandy loam (Lundblad, 2015; Paulsson et al., 2015) and the soil density, field capacity, saturation, permanent wilting point, and plastic limit of sandy loam described in (Witney, 1988) was assumed adequate and used. Weather data on monthly mean air temperature, number of daily sunshine hours, and hourly precipitation were obtained from the meteorological station at the Visby Airport on Gotland, Sweden (57°66′N 18°34′E). Even though for wind power production and electricity prices data from 2017 was considered, to model the agricultural H_2 demand, data of precipitation, air temperature, and sunshine hours from 2016 were considered since they better represented average values in the region for the period 1989–2018 (SHMI, 2020). The H_2 demand during crop harvesting was modeled based on 28% of total fuel demand in a cereal farm according to Safa et al. (2010). The instantaneous power demand for the FCAM and the refuelling station was measured separately and were both assumed to be linear average values. The average refuelling time considered was 0.32 h and the refuelling station was assumed to have a constant H_2 flow for the duration. The input values used to simulate the H_2 demand of FCAM are shown in **Table 3**.

H_2 demand of FCMV was estimated for an average driving of 35,000 km/year with a diesel-equivalent consumption of 4.43 L/100 km. The total consumption of 1,825 L/year (8.86 L/day) was equally distributed throughout the year and added to the H_2 demand of FCAM when applicable (see *Agricultural H_2 Demand*).

TABLE 2 | Summary of the different agricultural PtH_2 cases assessed.

Cases	Type	Total farm area	Wind power capacity	PtH_2 plant	H_2 demand
1	Single-farm	300-ha	20 MW	Single-user	FCAM
2a	Two-farms	600-ha	40 MW	Multi-user	FCAM
2b	Two-farms	600-ha	40 MW	Multi-user	FCAM and FCMV[a]
3a	Four-farms	1,200-ha	80 MW	Multi-user	FCAM
3b	Four-farms	1,200-ha	80 MW	Multi-user	FCAM and FCMV[b]

[a]*8.86 L of diesel-equivalent per day to fuel two fuel cell minivans (FCMV); FCAM–fuel cell agricultural machinery.*
[b]*17.72 L of diesel-equivalent per day to fuel four FCMV.*

By-Products Recovery

As the primary aim of the current study is to investigate H_2 production on-demand, by-products production is not optimized. However, it is nevertheless possible to recover the produced WH and O_2 for individual end-use applications. To valorize the WH stream, the size of the greenhouse was varied from 1,000 to 10,000 m^2 for tomato production according to the rated power of each simulated electrolyser size (50–500 kW). A water tank (heat capacity of 70 kWh/m^3; 5% whole system thermal losses assumed) with up to 24 h of full load capacity is used to account for short-term imbalances between heat supply and demand such as daily fluctuations during summertime (Novo et al., 2010; Guelpa and Verda, 2019). Along with the varying greenhouse size, different sizes of water tanks were also considered from 3 to 30 m^3 with a specific investment cost of 40 €/m^3 (Guelpa and Verda, 2019). More information about the heat demand estimation can be found in **Figure A1** in Appendix A.

For the on-site use of O_2, it was considered that all assessed farm configurations are combined with a 2,500 m^3 tank for rainbow trout cultivation where O_2 is injected for controlling the dissolved oxygen levels in the water. A stock density of 15 kg/m^3 was applied with an average specific O_2 consumption of 350 mg O_2/kg/h (Boyd, 2011; Woynarovich et al., 2011). As the produced O_2 from the electrolyser can only offset 23–27% of the total demand for fish farming, each tank is equipped with a dedicated O_2 generation system based on pressure swing adsorption (PSA) technology with a power consumption of 1.1 kWh per m^3 of O_2 (85% v/v) (Aquaculture Technology, 2020). Given an electricity tariff of 100 €/MWh (regulated market), those characteristics result in an O_2 production cost of around 0.19 €/kg. Hence, this value is further used to monetize the O_2 production from the electrolyser.

Power-to-Hydrogen Model and Optimization Procedure

The PtH_2 model was implemented in the Matlab-based Simulink environment version R2019b (MathWorks, USA). Individual equations are discretized for a fixed step size (sampling time) of 1 h. It is based on variable hourly values of wind power production, day-ahead spot market price, and fuel demand. The PEM electrolyser was modeled in combination with a compressed gas storage system to assist H_2 production and delivery on-demand. The model calculates H_2, WH, and O_2 production as well as run hours and total electricity cost. The decision whether the electrolyser should enter into operation is

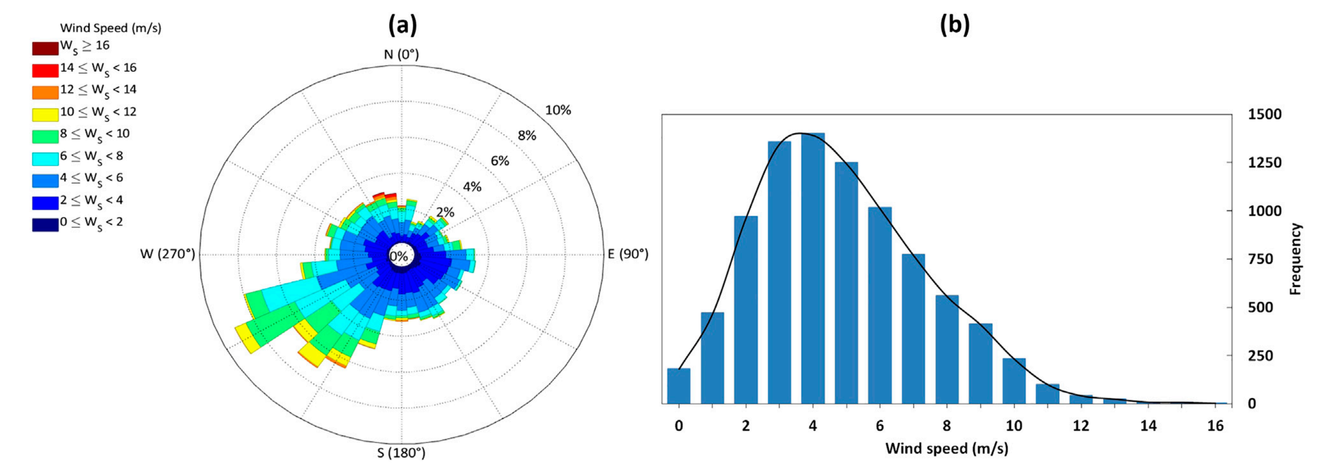

FIGURE 3 | Wind rose **(A)** and wind speed frequency distribution **(B)** at the Visby Airport on Gotland, Sweden.

dependent on the amount of H_2 available in the gas storage and the availability of wind power to run the electrolyser on full-load as described below (**Eq. 2**):

$$E_i = \begin{cases} 1 & \textit{if } V_{H_2,i} < V_{H_2,\max} \text{ and } W_{wind,i} \geq W_{elec} \\ 0 & \textit{else} \end{cases} \tag{2}$$

where E_i - electrolyser operation mode (binary), $V_{H_2,i}$ - gas storage volume in each hour i (m^3 at 500 bar), $V_{H_2,max}$ - available gas storage size (m^3 at 500 bar), $W_{wind,i}$ - wind power production in each hour i (MWh), W_{elec} - hourly power consumption of the electrolyser on full load (MWh).

H_2 production in each hour ($m_{H_2,i}$) is calculated based on the power consumption of PEM electrolysis in 2020 and 2030 (**Eq. 3**):

$$m_{H_2,i} = E_i \cdot W_{elec} \cdot \frac{\rho_{H2}}{W_{H_2,i}} \tag{3}$$

where ρ_{H2} - H_2 density (0.08988 kg/m^3 at STP), $W_{H_2,i}$ - specific power consumption during operation mode (4.6–4.9 kWh/m^3 H_2 at STP).

O_2 production ($m_{O_2,i}$) is calculated based on hourly H_2 production and the molar mass of H_2O, H_2, and O_2 (**4** and **5**):

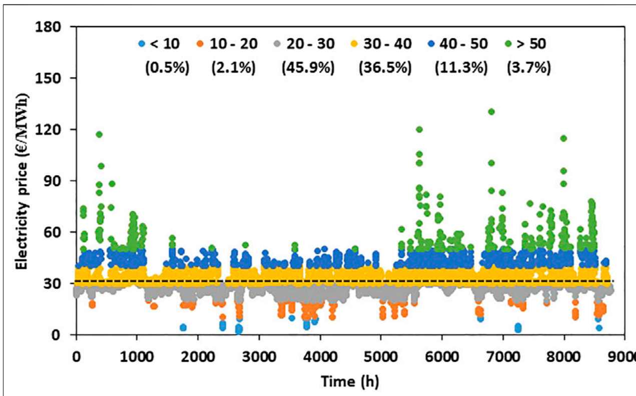

FIGURE 4 | Day-ahead price distribution in the spot market of the Nord Pool for SE3 region. Note: Dotted line represents the average price in the year.

$$m_{H_2O,i} = \frac{m_{H_2,i}}{r_{H_2}} \tag{4}$$

where $m_{H_2O,i}$ - H_2O consumption in each hour i (kg), r_{H_2} - molar mass ratio of H_2/H_2O (0.111907).

$$m_{O_2,i} = m_{H_2O,i} \cdot r_{O_2} \tag{5}$$

where r_{O_2} - molar mass ratio of O_2/H_2O (0.888093).

Waste heat production in hour i ($W_{heat,i}$) is calculated as a fraction of the consumed power during operation mode (**Eq. 6**):

$$W_{heat,i} = W_{H_2,i} \cdot f_{heat} \tag{6}$$

where f_{heat} - fraction of electrolyser's power consumption that becomes available heat (0.171).

The run hours of the system per year (R_{ON}) is defined as the sum of hourly events that satisfies the condition needed to the electrolyser enter on operation mode (**Eq. 7**):

$$R_{ON} = \sum_{i=1}^{8760} E_i \tag{7}$$

The costs associated with electricity use during the electrolyser operation ($C_{elec,i}$) are based on wind power consumption ($W_{H_2,i}$) and from the grid for safety infrastructure (W_{safe}) as follows:

$$C_{elec,i} = T_{spot,i} \cdot W_{H_2,i} \cdot \frac{m_{H_2,i}}{\rho_{H2}} + T_{grid} \cdot W_{safe} \cdot \frac{P_N}{1.074} \tag{8}$$

TABLE 3 | Inputs used for simulation of H_2 demand of the fuel cell agricultural machinery (FCAM).

Parameters	Value	Unit
Effective vehicle power	100	kW
Charger power	1,000 (30)	kW (kg h^{-1} H_2)
Rated fuel tank energy content[a]	323 (8.2)	kWh (kg H_2)
Number of refuelling stations	1	(—)
Daily working time	10	(h)
Tank-to-wheel efficiency[b]	50	(%)

[a]*NHA, 2012.*
[b]*Moreda et al., 2016.*

where $T_{spot,i}$ - is the day ahead spot market price in each hour i of the electrolyser operation (€/MWh), T_{grid} - is the fixed tariff for grid-based power (100 €/MWh), P_N - electrolyser's nominal rated power (MW)

The yearly costs to keep the electrolyser on cold standby (C_{cold}) during non-operating hours is described in **Eq. 9** as follows:

$$C_{cold} = T_{grid} \cdot W_{cold} \cdot \frac{P_N}{1.074} \cdot (8760 - R_{ON}) \tag{9}$$

The power consumption during cold standby and for safety infrastructure is based on a 1.074 MW plant and is proportionally adjusted to each size of electrolyser assessed (Frank et al., 2018). To allow gas storage at 500 bar, H_2 is compressed requiring 2.2 kWh/kg H_2 (W_{comp}) (Linde, 2014). The costs associated with H_2 compression ($C_{comp,i}$) in each hour i are described in **Eq. 10** below:

$$C_{comp,i} = T_{spot,i} \cdot W_{comp} \cdot m_{H_2,i} \tag{10}$$

Finally, the total electricity cost of the PtH_2 plant (C_{total}) is based on costs associated during the electrolyser operation ($C_{elec,i}$), H_2 compression ($C_{comp,i}$) and to keep the electrolyser on cold standby (C_{cold}) **(Eq. 11)**:

$$C_{total} = \sum_{i=1}^{8760} \left(C_{elec,i} + C_{comp,i} \right) + C_{cold} \tag{11}$$

To determine the optimal plant configuration a total number of 256 simulations were run for each case assessed. Each simulation corresponded to a combination of electrolyser size between 50 and 500 kW (30 kW increments) and gas storage capacity between 10 and 50 m^3 (2.66 m^3 increments). For each plant configuration, specific CAPEX (€/kW), capacity factor, the average price paid for the electricity, and the $LCOH_2$ were calculated and used for assessment. To verify whether the PtH_2 plant configurations were fulfilling the consumers' fuel requirement, the delivery of H_2 on-demand was considered a mandatory criterion. The characteristic dependencies of different plant configurations on each performance indicator were visualized using Matlab function contour 3-days plot (MathWorks, USA). For each case assessed, the combination of electrolyser size and gas storage capacity that resulted in the lowest $LCOH_2$ and simultaneously fulfills H_2 demand was considered the optimal plant configuration.

Economic Assessment

The economic performance of the system was assessed based on two economic indicators, namely the $LCOH_2$ and equivalent annual cost (EAC). While the $LCOH_2$ is used to optimize the PtH_2 plant configuration in terms of electrolyser size and H_2 storage capacity, the EAC is used to compare the H_2 system with a conventional diesel-fueled one. To determine the EAC, the net present value (NPV) is first calculated as follows **(Eq. 12)**:

$$\text{NPV} = -\text{CAPEX} + \sum_{y=0}^{n} \frac{\text{NCF}_y}{(1+k)^y} \tag{12}$$

where CAPEX is the capital expenditures of the PtH_2 or diesel system; k is the discount rate estimated at 6.5% per year for onshore wind projects in Nordic countries (Thornton, 2019); y is the 25 years lifespan of the project.

The net cash flow (NCF) is the operational expenditures subtracted by the land lease over the lifespan of the project as per **Eq. 13:**

$$\text{NCF}_y = (\text{Heat use} + \text{O}_2\text{ use} + \text{Land lease}) - \text{OPEX}_y \tag{13}$$

where Heat use is annual savings produced by utilizing the electrolyser's waste heat as opposed to traditional heating at a conservative value of €75/MWh (Wiederholm et al., 2018); O_2 use annual savings produced by utilizing the electrolyser's waste O_2 at a saving of 0.19 €/kg; Land lease is the yearly income by leasing the land for wind power production (6,000 €/MW per year) (McGreevy, 2013); $OPEX_y$ is the yearly operational expenditures of the PtH_2 or diesel systems. Here, fixed as well as variable costs such as electricity and water for the PtH_2 plant and fuel consumption for the diesel system are considered. The latter is assumed to be equivalent to the H_2 demand in energy units multiplied by the tank-to-wheel efficiency ratio between fuel cell and diesel vehicles (50%/30%) (Moreda et al., 2016).

Different diesel prices are considered to depict the influence of agricultural diesel tax relief as well as a future fuel prices in Sweden. A summary of the different prices considered in the present study are shown in **Table 4**.

Finally, the EAC is calculated as the cost per year of owning and operating the PtH_2 and diesel-fueled agricultural systems over the lifespan of the project as follows **(Eq. 14)**:

$$\text{EAC} = \frac{\text{NPV}}{\frac{1-\frac{1}{(1+k)^y}}{k}} \tag{14}$$

The $LCOH_2$ is the breakeven selling price of the H_2 produced and is given by **Eq. 15** below:

$$\text{LCOH}_2 = \frac{\sum_{y=0}^{n} \frac{\text{costs in year y}}{(1+k)^y}}{\sum_{y=0}^{n} \frac{\text{kWh of H}_2\text{ produced in year y}}{(1+k)^y}} \tag{15}$$

All indicators are calculated in 2018 euros.

The timeline for relevant calculations includes a 3-year commissioning phase, 25 years of operation, and one-year decommissioning. Also, additional costs, such as land, permits, transport, site preparation, engineering, and design costs, grid connection as well as contingency were assumed to be equivalent to 10% of the electrolyser's CAPEX (Benjaminsson et al., 2013).The economic model does not consider reductions in electrolyser performance over time, however, component replacement costs are included in economic assessment (2 replacements over project's lifetime). Even though our study uses the most recent literature available, unavoidable uncertainties exist in capital expenditures (Schmidt et al., 2017). CAPEX and OPEX values of PEM electrolyser used in this study are shown in **Table 5**.

TABLE 4 | Description of the different diesel prices considered for assessment.

Carbon tax scheme	2020	2030
With carbon tax (retail price)	1.35 €/L (5.33 €/kg_{H2})[a]	1.62 €/L (6.40 €/kg_{H2})[b]
With carbon tax relief (agricultural use)	1.17 €/L (4.62 €/kg_{H2})[c]	1.40 €/L (5.53 €/kg_{H2})

[a]*Current diesel retail price on Gotland (Sweden) (Bensinpriser.nu, 2020).*
[b]*Approx. 20% increase (IVL, 2012).*
[c]*Tax relief on diesel consumption of 1,930 SEK/m^3 of diesel (Skatteverket, 2020).*

RESULTS AND DISCUSSIONS

H_2 Demand

As described in *Agricultural H_2 Demand*, H_2 demand was modeled for different farm cases which include FCAM, some also include FCMV. As an example, **Figure 5** shows the demand profile at the dispenser for case 2b where two farms share a PtH_2 plant to fuel their agricultural machinery and one FCMV each. As expected, H_2 demand for FCAM is highly seasonal, there is no demand during winter, extended parts of the summer, and some interim periods when no fieldwork is required. In contrast, H_2 demand of FCMVs occurs on a year-round basis, however, requiring much less energy than FCAM per refill. In fact, the total H_2 demand of the FCMVs in case 2b was just 28% of the total fuel demand.

When the PtH_2 plant is scaled-up to fulfill the H_2 demand of four farms including one FCMV each (case 3b), the fuel demand is double that seen in **Figure 4** with the same demand profile. Conversely, where a single farm operates a PtH_2 plant (case 1) FCAM demand is halved and FCMV is disregarded.

Optimization of H_2 Production

For the optimization of the PtH_2 plant, the electrolyser and storage capacity sizes were varied to find plant configurations that resulted in the lowest possible $LCOH_2$. This procedure was performed for each farm case as well as for different technological scenarios assessed (**Figure A2** in **Appendix B**). Again, case 2b (2020) is used as an example (**Figure 6**).

TABLE 5 | Capital expenditures (CAPEX), balance of the plant (BoP) and operational expenditures of the PtH_2 plant in different technological scenarios.

Costs		2020	2030
Type	Items		
PtH_2 plant	CAPEX of PEM electrolyser (€/kW)[a]	970	530
	BoP[b]	0.15	0.15
	OPEX[b]	0.04	0.032
	Replacement[b]	0.2	0.2
	H_2 storage (€/kg)	600	400
	H_2 dispenser (€)	80,000	52,000
Diesel system	Diesel dispenser (€)	5,000	5,000
Agricultural machinery	CAPEX of diesel tractor (€)	60,000	60,000
	CAPEX of fuel cell tractor (€)	100,000	100,000

Note. All values obtained from *de Bucy et al., 2016; Schmidt et al., 2017; McDonagh et al., 2018; Zauner et al., 2019; and Ulleberg and Hancke, 2020.*
[a]CAPEX of PEM electrolyser is based on a 5 MW plant and scale-effect was calculated based on 0.75 factor according to STORE&GO project *(Zauner et al., 2019).*
[b]*Fraction of CAPEX.*

Economies of scale are significant in the ranges examined and heavily influenced the economic performance of the agricultural PtH_2 plant (Zauner et al., 2019). However, as shown in **Figure 6B**, increasing electrolyser sizes also led to lower capacity factors. Such behavior is explained by the plant being driven according to the specific H_2 demand, thereby increasing electrolyser capacity did not necessarily result in higher H_2 production. Previous studies on electrofuels production showed that the number of running hours of the plant and the price paid for the electricity were the most important factors to minimize the production costs for a fixed capacity (McDonagh et al., 2019; Janke et al., 2020). In the present study, as the average price paid for the electricity varied less than 10% among all simulated conditions, it was indeed the capacity factor that most influenced the H_2 production costs. For instance, in case 2b (2020) the lowest $LCOH_2$ was found for a plant with a 140 kW of electrolyser size and 15 m^3 (500 bar) of storage capacity (i.e., equivalent to 11 days of full-load operation). This plant configuration resulted in 3,060 h/year of operation and it was able to produce H_2 at a cost of 15.87 €/kg. When the H_2 demand of FCMN is disregarded (case 2a–2020), a comparable PtH_2 plant would operate 11% less (2,715 h/year), which in turn results in around 6% higher H_2 production costs. In contrast, if the electrolyser size would be reduced to lower than 140 kW, the number of operating hours would increase, which in theory could potentially reduce the production costs. As observed in **Figure 6B**, however, if smaller electrolysers are used H_2 is not delivered on-demand, thus excessively small electrolysers are not considered suitable for farm operations even if coupled to large storage capacities (expensive option).

In fact, due to the highly seasonal fuel demand and relatively high cost of additional storage capacity, it is challenging to design a PtH_2 plant with sufficient run hours able to truly minimize the $LCOH_2$. A previous study on $PtCH_4$ showed that at least 5,000 operating hours per year (57% capacity factor) would be required, and values lower than 4,000 h/year would likely result in prohibitive production costs (McDonagh et al., 2019). For case 2b (2020) the $LCOH_2$ of 15.87 €/kg is equivalent to a diesel price of 4.02 €/L which is indeed prohibitive when compared to the assumed diesel retail price of 1.35 €/L. Such diesel price includes a carbon tax of 110 €/tCO_2 applied for fossil fuel consumption. In countries like Sweden where farmers pay less for consuming fossil fuel due to the relief on the existing carbon tax, the adoption of alternative fuels by farmers becomes even more challenging since the real diesel price paid by farmers is around 1.17 €/L.

In case farmers organize themselves in a small cooperative where four farms share the same PtH_2 infrastructure to supply fuel for their agricultural machinery and one FCMV in each

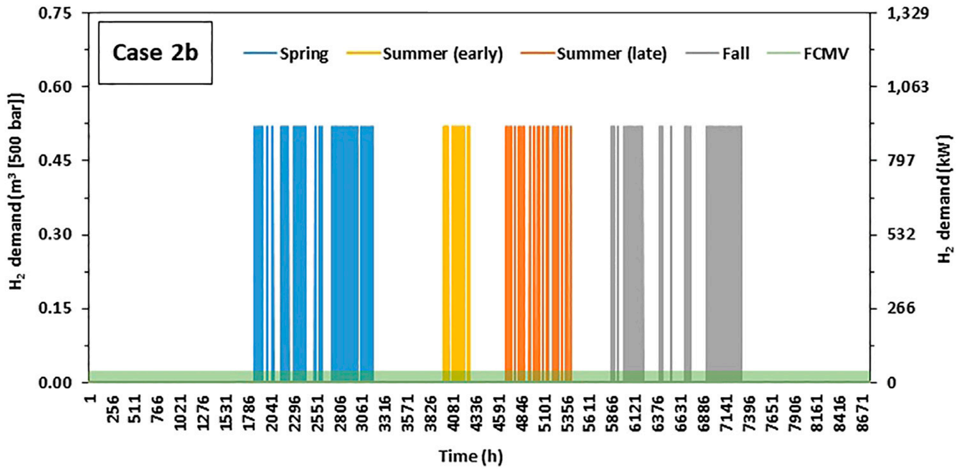

FIGURE 5 | H_2 demand profile of the cereal farm system for the case 2b. Note: Detailed description of the agricultural activities carried out in each season is provided by Lagnelöv et al. (2020); FCMV - fuel cell minivan.

farm (case 3b), the system is up-scaled to an optimal configuration of 290 kW electrolyser and 26 m^3 (500 bar) of storage capacity. Even though this higher H_2 demand does not necessarily result in major changes in the capacity factor of the plant, the specific CAPEX is reduced by 17% compared to sharing the infrastructure with just two farms (case 2b), which in turn proportionally reduces the H_2 production costs (**Table 6**).

New composite materials for compressed H_2 storage and reduced use of noble metals like platinum and titanium in PEM electrolysis will result in lower costs in the future (Schmidt et al., 2017; Moradi and Groth, 2019). As no changes in optimal plant configurations were found in 2030 compared to 2020, these technological developments are considered the main reason for the 30% reduction in $LCOH_2$ observed. Interestingly, a previous study from our group based on H_2 production without demand constraints, showed a lower reduction of 18% in production costs when comparing 2020 and 2030 technological scenarios (Janke et al., 2020). In that case, the higher capacity factor of the electrolyser (≥75%) increased the total expenses with electricity purchase, thereby reducing the effect of CAPEX on the $LCOH_2$.

Effect of By-Products Recovery

The PtH_2 plant produces and delivers H_2 according to the demand of FCAM and FCMV, however, the process of water electrolysis also results in O_2 production mediated by an exothermic reaction (**Eq. 1** described in *System Description*). As PEM electrolysers are operated under controlled temperature (50–80°C), a water-based cooling system needs to be integrated to avoid overheating of the cell (>100°C), thereby also allowing the recovery of low-temperature waste heat (Buttler and Spliethoff, 2018). The feasibility of valorizing these by-products depends on local demand. For instance, our farm includes intensive tomato cultivation in a greenhouse, which requires temperature control for year-round production. In this case, it is assumed that the electrolyser's cooling system could be integrated to the heating system of the greenhouse, offsetting the heat required from conventional sources (Wiederholm et al., 2018). Furthermore, O_2 use in aquaculture has gained attention in recent years, in particular in recirculating aquaculture systems that require high levels of dissolved oxygen to allow high production densities. As O_2 would be usually generated on-site via energy-intensive PSA systems, water electrolysis could partly supply O_2 to aquaculture offsetting costs associated with the oxygenation process. Both WH and O_2 valorization would positively impact the economic performance of the PtH_2 plant. Such benefits in terms of $LCOH_2$ reduction are shown in **Figure 7**.

Independent of the case and/or year assessed recovering O_2 showed to be more valuable compared to WH. On average, a reduction by 12% on the $LCOH_2$ was possible by recovering O_2, while WH was able to reduce the production costs by approximately 5%. This is mostly explained by the large quantities of O_2 generated by the water electrolysis process, i.e., 88% of H_2O mass becomes O_2. Thus, assuming a price of 0.19 €/kg, O_2 recovery substantially improves the economic performance of the process. When both O_2 and WH are valorized, the $LCOH_2$ is reduced on average by 17%.

However, diesel is still cheaper than H_2 in all cases and years at the given prices. For instance, in 2020 the lowest $LCOH_2$ found in case 3b (11.44 €/kg) was between 2.14 and 2.47 times higher than diesel with and without carbon tax respectively. In 2030, when diesel prices are expected to be 20% higher and H_2 production costs 23% lower than in 2020 (case 3b with WH and O_2 recovery), such differences are reduced to 1.15–1.33 times higher than diesel depending on the carbon tax scheme considered.

As clearly observed, purchasing diesel is cheaper than on-farm H_2 production, for all PtH_2 cases and technological scenarios considered. However, due to significant differences in terms of tank-to-wheel efficiency and purchase costs between FCAM and conventional diesel agricultural machinery, further analysis is required to understand the competitiveness of small-scale H_2 production for farming activities.

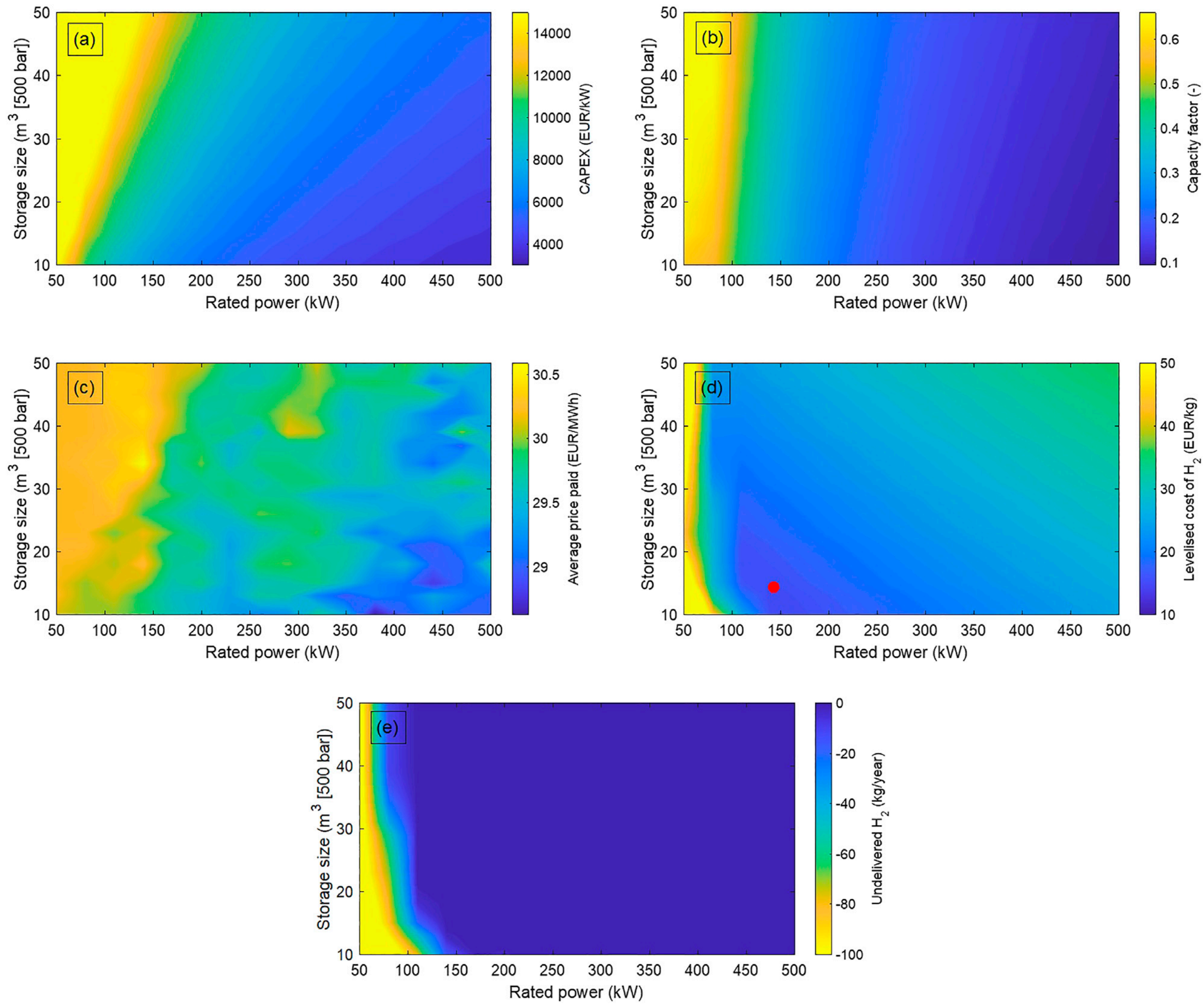

FIGURE 6 | Results of electrolyser and storage capacity optimization for case 2b in 2020. **(A)** specific capital expenditures (CAPEX); **(B)** capacity factor; **(C)** average price paid for the electricity; **(D)** levelized cost of H_2 ($LCOH_2$); **(E)** H_2 delivery check. Note: Red dot shows the optimal plant configuration to minimize $LCOH_2$.

Equivalent Annual Cost

The equivalent annual cost (EAC) was assessed as an additional economic indicator to understand the H_2 system from the farmers' perspective. The EAC is used to compare the cost of owning fuel cell or diesel vehicles over the lifetime of the PtH_2 plant. In addition, a scenario where farmers finance H_2 production and use by means of leasing land to wind power project developers is also considered. Such a business model is considered advantageous for both parties: 1) farmers obtain additional revenues by leasing their land for wind power production; 2) wind power project developers potentially enhance their wind power production by selling curtailed electricity to farmers; 3) farmers can locally produce clean fuel to decarbonize their activities, and 4) support for the wind farm will likely be much greater with local involvement. The EAC according to the different farm cases and technological scenarios assessed are found in **Figure 8**.

Important differences were observed among the farm cases, in which sharing the PtH_2 plant between two farms reduced the EAC by 21% on average, and sharing the PtH_2 plant among four farms reduced annual costs by 27%. In contrast, no major benefits were found if farmers share the same diesel refueling infrastructure since the CAPEX of the diesel system is considerably lower than the H_2 one. Nevertheless, EAC values associated with H_2 production and use were always higher than conventional diesel farming for the period 2020 unless land lease revenues are counted.

Similarly to the $LCOH_2$, the EAC of the H_2 system will be considerably lower in 2030. In this case, annual costs would be around 30% lower compared to 2020 values. In the meantime, diesel prices are expected to increase by around 20%, reaching values between 1.40 and 1.62 €/L depending on the carbon tax scheme considered. Due to these factors, the EAC of the H_2 system becomes competitive with diesel, except for case 1 which

TABLE 6 | Results of PtH_2 plant optimization according to different cases assessed.

Year	Case	Optimal plant configuration		CAPEX (€/kW)	Capacity factor	Av. Price paid (€/MWh)	$LCOH_2$ (€/kg)
		Electrolyser (kW)	H_2 storage (m^3 [500 bar])				
2020	1	50	13	14,620	47%	30.35	21.20
	2a	140	13	7,914	31%	29.88	16.89
	2b	140	15	8,384	35%	30.05	15.87
	3a	260	29	7,719	34%	30.03	15.31
	3b	290	26	6,935	34%	29.74	13.82
2030	1	50	13	10,089	47%	30.35	14.82
	2a	140	13	5,398	31%	29.88	11.65
	2b	140	15	5,732	35%	30.05	11.03
	3a	260	29	5,329	34%	30.03	10.87
	3b	290	26	4,806	34%	29.74	9.77

Note. $LCOH_2$ without waste heat (WH) or O_2 recovery.

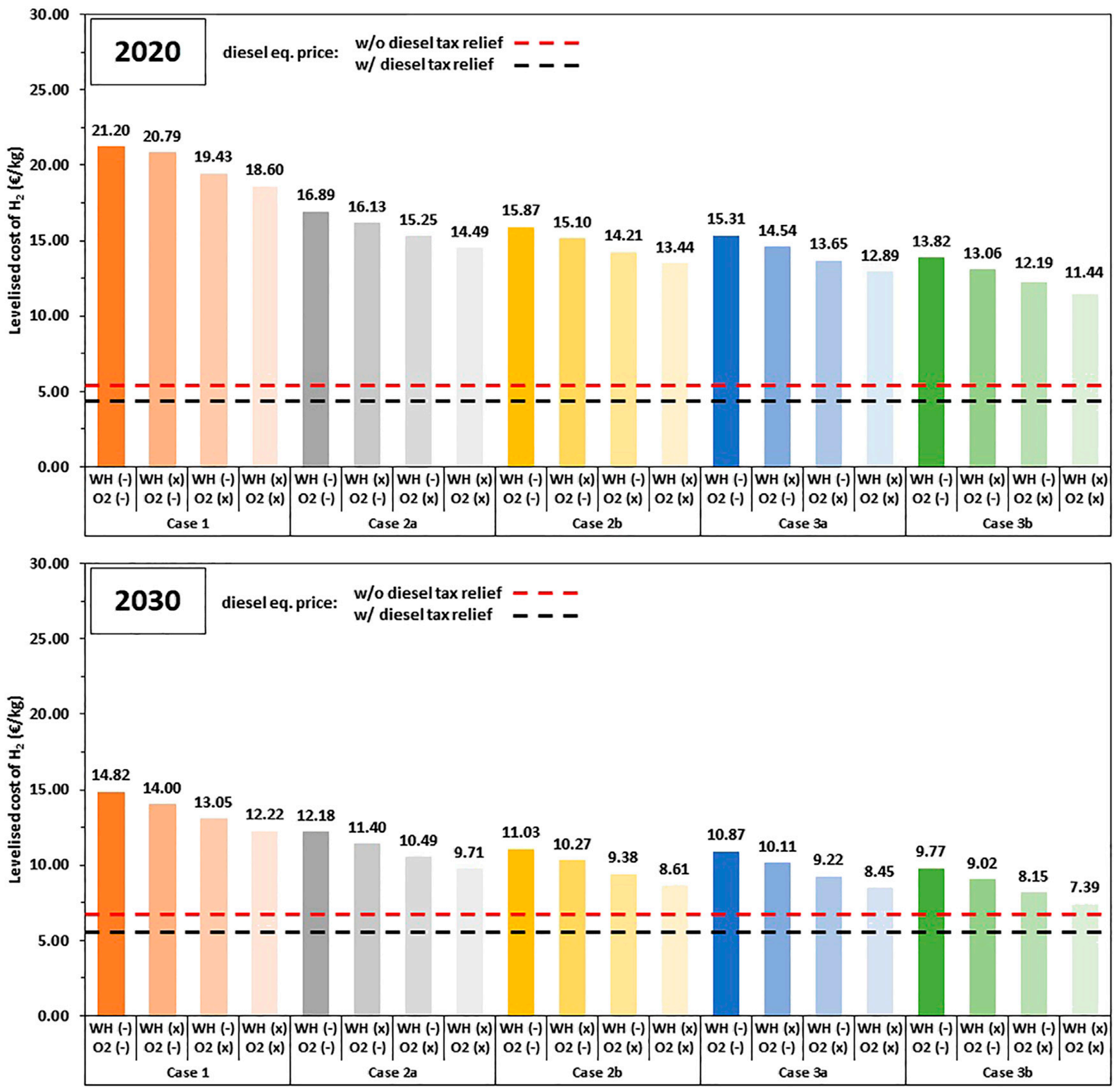

FIGURE 7 | Effect of by-products recovery on the levelized cost of H_2 ($LCOH_2$) according to the different cases assessed. Note: Red dotted lines represent the diesel equivalent price without tax relief (2020–1.35 €/L or 5.33 €/kg H_2; 2030–1.62 €/L or 6.40 €/kg H_2); black dotted lines represent the diesel equivalent price with tax relief (2020–1.17 €/L or 4.62 €/kg H_2; 2030–1.40 €/L or 5.53 €/kg H_2); WH–waste heat; O_2–oxygen; (-) without; and (x) with.

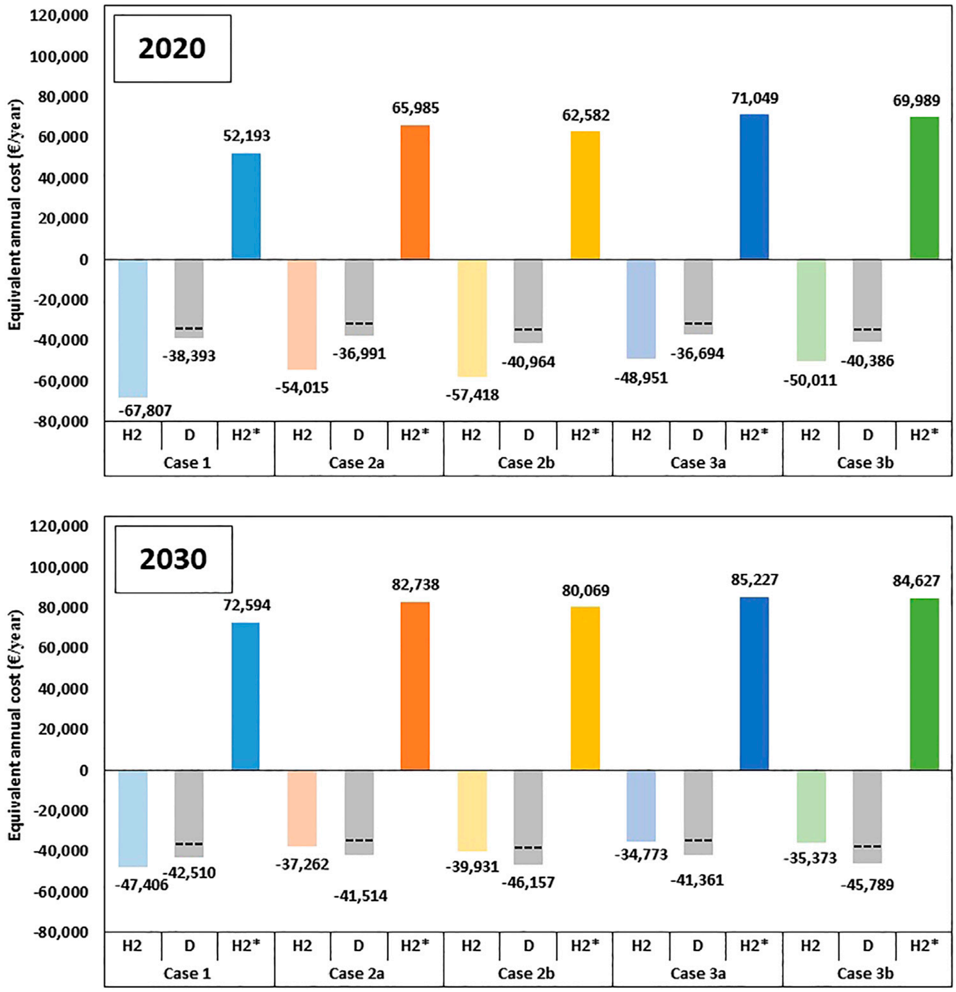

FIGURE 8 | Equivalent annual cost (EAC) of the different cases assessed. Note: H2 means PtH_2 without land lease revenues; D means diesel-fueled farm; H2* means PtH_2 with land lease revenues; Values are presented per farm in Cases 2a,b, and 3a,b; black dotted lines represent EAC of diesel with tax relief; EAC values of PtH_2 cases do not consider waste heat (WH) or O_2 recovery.

still will be more expensive. For case 2a, H_2 becomes cheaper than diesel if farmers are not entitled to carbon tax relief on diesel consumption. For all remaining cases in 2030 H_2 shows lower or equal EACs than diesel. Unsurprisingly, the case that presented the lowest EAC (3a–2030, no FCMV) was not the same case that showed the lowest $LCOH_2$ (3b–2030, inc. FCMV). This is explained by the $LCOH_2$ being inversely proportional to the amount of H_2 produced **(Eq. 5)** which increases with the inclusion of FCMV demand, while the EAC is only marginally influenced by production via the NPV **(Eq. 2-4)**. Thus, by adding the H_2 fuel demand of FCMV, the increase in cost is greater than the savings produced from having H_2 production, however, we did not compare this to diesel minivans as FCAM was the focus of this study.

When the revenues for leasing the land to wind power project developers are taken into account (6,000 €/MW/year), a major impact on the EAC is observed in favor of the H_2 system. In this case, instead of having costs associated with agricultural machinery, farmers would have annual gains by operating the PtH_2 plant in all farm cases and technological scenarios assessed. In cases where H_2 production and use is less competitive than diesel, only a minor share of the land lease revenues would be required to make H_2 competitive with diesel. For instance, under the current technological scenario, between 10–26% (600–1,560 €/MW/year) is needed to finance H_2 production and use. In the 2030 scenario, only case 1 requires additional assistance from land lease revenues to make it competitive with diesel. In this case, the fraction of land lease revenues needed would be reduced from 26% to just 8% (498 €/MW/year).

Carbon Abatement Cost

The implementation of a farm-based PtH_2 plant results in carbon emission reductions from different sources, namely direct fossil fuel displacement by H_2, power consumption from the grid by recovering O_2 from the electrolyser, and reductions in district heating use also by recovering WH from the electrolyser. As the latter two are dependent on local characteristics such as variable emission factor from the grid and use of fossil fuel in district

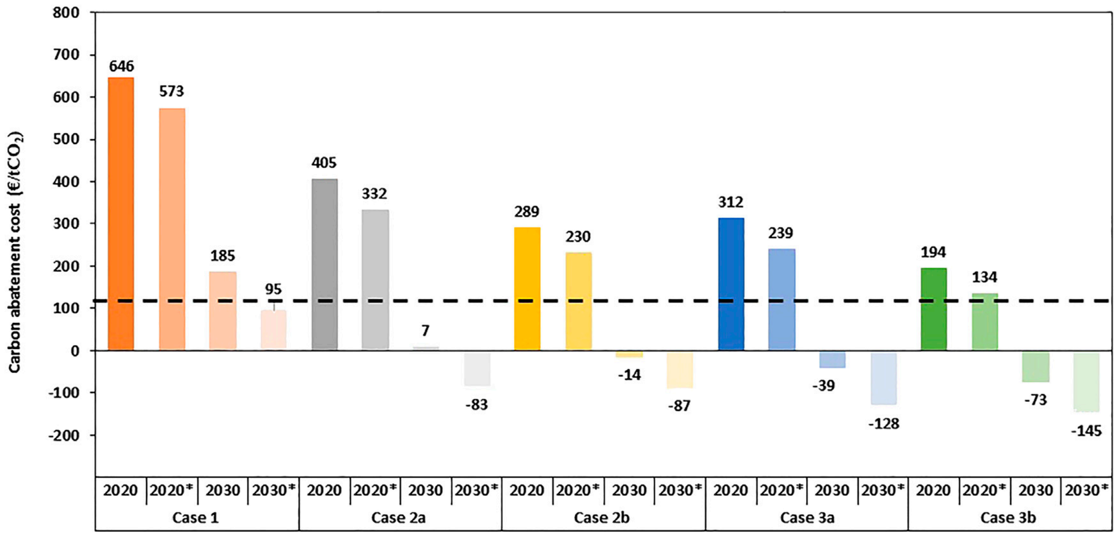

FIGURE 9 | Carbon abatement cost of the different cases assessed. Note: * means without diesel tax relief; black dotted line represents the carbon tax in Sweden (2020).

heating systems, a simplified approach to calculate the cost of carbon mitigation was performed solely focusing on diesel displacement by the produced H_2.

Considering a diesel consumption of 19,446 L/farm/year without FCMV, 27,131 L/farm/year with FCMV and the diesel emission factor of 2.64 $kgCO_2/L$, the carbon emission reductions provided by the PtH_2 plant could be estimated. In addition, the difference in EAC between H_2 and diesel with and without carbon tax relief was used to calculate the carbon abatement cost of each case in different technological scenarios (**Figure 9**).

It is possible to observe that under the current technological scenario without land lease revenues the carbon abatement cost is considered high, with values above 100 €/tCO_2. The case 3b showed, however, the lowest carbon abatement cost in 2020 with values close to the current carbon tax in Sweden (110 €/tCO_2), in particular if the diesel tax relief entitled to farming activities would be excluded. In fact, state subsidies and taxes often influence positively or negatively the cost efficiency of carbon abatement costs of different mitigating measures (Eory et al., 2018). For instance, incentives for the production and use of H_2 could reduce its carbon abatement costs, but the existing tax relief on fossil fuel consumption prevents the adoption of low carbon fuels by the agricultural sector in Sweden.

In 2030, the carbon abatement costs are negative in most farm cases examined. Negative carbon abatement costs have been previously reported for different activities such as lighting switch, methane recovery from landfills, retrofit insulation in buildings, among others (McKinsey and Company, 2009). They owe negative values due to the advantage of having higher economic benefits than their implementation costs. In our case, this is translated by lower annual costs than diesel farming in most of 2030 cases. Such a favorable situation is not only due to the expected technological developments but also due to the 20% increase in diesel prices in the future. Thereby, emphasizing the importance of the price paid for diesel on the development of efficient climate protection strategies by policymakers.

Alternative Demand Profiles

As discussed in *H_2 Demand* and *Optimization of H_2 Production*, H_2 demand has a major impact on the optimal plant configuration and performance of the H_2 system. Where additional H_2 consumers could be integrated, resulting in alternative demand profiles, significant improvements in terms of production costs could be achieved. For instance, in case 2b (2030) the $LCOH_2$ of 11.03 €/kg is equivalent to a diesel price of 2.79 €/L, which is 2.4 times more expensive than currently found in retailers, including diesel tax relief. Such high production costs can be largely attributed to the low capacity factor of the PtH_2 plant. If the H_2 demand of FCMV in case 2b were to be multiplied by 10, i.e., 88.6 L of diesel eq. per day, a PtH_2 plant with an electrolyser size of 200 kW and 18 m^3 (500 bar) of capacity storage would be able to fulfill the demand of FCAM and FCMV, and at the same time operate during 4,241 h/year (48% of capacity factor). The PtH_2 plant, thus, could lower H_2 production costs to 7.04 €/kg in 2030, reaching a diesel equivalent price of 1.78 €/L (without by-products recovery). However, such a case is more akin to a small commercial filling station forecourt than a farm-based system and would require significant conversion of the local fossil fuel fleet to hydrogen fuel cells, or a medium-sized captive fleet.

Beyond sharing facilities across multiple farms as examined in this study, other farm types could be investigated for suitability for conversion to FCAM. In this case, ley crops for a dairy farm could show a more distributed H_2 demand throughout the year, reducing gas storage requirements as well as allowing the PtH_2 plant reach higher capacity factors. In addition, if these type of crops were integrated into a small pool of cereal-based farms sharing the same H_2 production infrastructure, the seasonality of fuel demand observed in the current study would certainly be reduced, potentially resulting in better economic performances.

Ultimately, strategies similar to a demand-side management approach could be applied even to farmers sharing the same PtH_2 plant with the same rotating crop system (e.g., present study). In this case, farmers could slightly adapt their agricultural operations to the availability of H_2, in particular during fall for plowing operations. Such strategy is considered a key aspect to improve the economic performance and it should be addressed in future studies on small-scale green H_2 production for agricultural applications.

Alternatively, H_2 surplus to FCAM demand could also be injected into agricultural biogas plants in a so-called *in-situ* biomethanation concept (Voelklein et al., 2019). Such synergies with agricultural biogas plants could be explored in different ways: 1) to increase biomethane output of biogas plants by reacting H_2 with CO_2; and/or 2) to use H_2 to partly displace costly energy crops as substrate like maize silage while keeping the same energy output of the biogas plant. Both concepts would increase the capacity factor of electrolysers and potentially decrease the costs of biogas production. However, care must be taken to ensure that the value of the methane-based H_2 and the economies of scale it allows for are greater than the sum of the additional costs.

Small-scale Haber-Bosch process (minimum of 1.5 MW) for ammonia fertilizer production could also be explored to provide an alternative demand for H_2 in the agricultural sector (Proton Ventures, 2018). This could quickly become the main demand for H_2 and would provide the required economies of scale to result in a more competitive H_2 either as fuel or platform for PtX processes.

CONCLUSIONS

This study examined the potential costs of an optimized system designed predominately to replace diesel-powered agricultural machinery with that powered by hydrogen (H_2) fuel cells. Several scenarios or cases were examined which included the addition of fuel cell light-duty vans, the sharing of H_2 facilities across neighboring farms, and valorization of the by-products (oxygen and waste heat). Results are presented in terms of levelized cost of hydrogen ($LCOH_2$), equivalent annual cost (EAC) to the farmer (consumer), and carbon abatement cost. Even though sharing the same H_2 facility among four farms decreased the $LCOH_2$ by 28% and by adding fuel demand for delivery vans further decreased production costs by 35%, given the current cost of diesel and associated carbon taxes, H_2 is not competitive in 2020. However, anticipated reductions in H_2 costs coupled with increases in diesel prices mean that by 2030 H_2 fuel cells may represent an economic option in many cases. Therefore, the carbon abatement costs varied drastically from −145 €/tCO_2 when H_2 becomes competitive with diesel in 2030, up to 646 €/tCO_2 in 2020. Nevertheless, when a PtH_2 plant is financed by the land lease revenues from a wind farm, H_2 becomes more competitive than diesel in all analyzed scenarios. Managing the demand profiles to decrease H_2 storage requirements and/or introducing an additional demand like for ammonia fertilizer production are effective strategies to reduce costs and should be addressed in future studies on H_2 production for low carbon agriculture.

DATA AVAILABILITY STATEMENT

All relevant data is contained within the article: The original contributions presented in the study are included in the article/supplementary material, further inquiries can be directed to the corresponding author.

AUTHOR CONTRIBUTIONS

LJ: Conceptualization, Methodology, Software, Validation, Formal analysis, Investigation, Data curation, Writing–original draft, Writing–reviewing and editing, Visualization. SM: Conceptualization, Methodology, Software, Validation, Formal analysis, Investigation, Writing–original draft, Writing–reviewing and editing. SW: Methodology, Software, Validation, Writing–reviewing and editing. DN: Conceptualization, Methodology. PH: Conceptualization. ÅN: Conceptualization, Writing–reviewing and editing, Supervising.

ACKNOWLEDGMENTS

The authors would like to acknowledge Oscar Lagnelöv for providing the required data on fuel demand of agricultural machinery and Gabriel Åkerman for having initiated the development of PtH_2 model.

REFERENCES

Linde. AG-Gases Division (2014). *The Ionic compressor 50.* Pullach (Germany).

Allman, A., and Daoutidis, P. (2018). Optimal scheduling for wind-powered ammonia generation: effects of key design parameters. *Chem. Eng. Res. Des.* 131, 5–15. doi:10.1016/j.cherd.2017.10.010

Allman, A., Daoutidis, P., Tiffany, D., and Kelley, S. (2017). A framework for ammonia supply chain optimization incorporating conventional and renewable generation. *AIChE J.* 63, 4390–4402. doi:10.1002/aic.15838

Apostolou, D., Enevoldsen, P., and Xydis, G. (2019). Supporting green urban mobility–the case of a small-scale autonomous hydrogen refuelling station. *Int. J. Hydrog. Energy.* 44, 9675–9689. doi:10.1016/j.ijhydene.2018.11.197

Aquaculture Technology (2020). Injection aerators for aeration, circulation, destratification and oxygenation. Available at: http://www.aquaculture-com.net/aeration.htm. (Accessed July 15, 2020).

Bailera, M., Peña, B., Lisbona, P., and Romeo, L. M. (2018). Decision-making methodology for managing photovoltaic surplus electricity through power to gas: combined heat and power in urban buildings. *Appl. Energy.* 228, 1032–1045. doi:10.1016/j.apenergy.2018.06.128

Bailera, M., Lisbona, P., Llera, E., Peña, B., and Romeo, L. M. (2019). Renewable energy sources and power-to-gas aided cogeneration for non-residential buildings. *Energy.* 181, 226–238. doi:10.1016/j.energy.2019.05.144

Benjaminsson, G., Benjaminsson, J., and Rudberg, R. (2013). Power-to-Gas: a technical review. Repport No.: 2013:284. Available at: http://sgc.camero.se/ckfinder/userfiles/files/SGC284_eng.pdf.

Bensinpriser.nu (2020). Diesel price on Gotland (Sweden). Available at: www.bensinpriser.nu (Accessed June 2, 2020).

Boyd, C. E. (2011). Dissolved oxygen requirements in aquatic animal respiration. Available at: https://www.aquaculturealliance.org/advocate/dissolved-oxygen-requirements-in-aquatic-animal-respiration/ (Accessed July 10, 2020).

Buttler, A., and Spliethoff, H. (2018). Current status of water electrolysis for energy storage, grid balancing and sector coupling via power-to-gas and power-to-liquids: a review. *Renew. Sustain. Energy Rev.* 82, 2440–2454. doi:10.1016/j.rser.2017.09.003

Byman, K. (2015). Locational study—Power to gas. Available at: http://www.energiforsk.se/program/energigasteknik/rapporter/locational-study-power-to-gas/.

Carroquino, J., Roda, V., Mustata, R., Yago, J., Valiño, L., Lozano, A., et al. (2018). Combined production of electricity and hydrogen from solar energy and its use in the wine sector. *Renew. Energy.* 122, 251–263. doi:10.1016/j.renene.2018.01.106

de Bucy, J., Lacroix, O., and Jammes, L. (2016). The potential of power-to-gas. Available online: https://www.enea-consulting.com/en/the-potential-of-power-to-gas/ (Accessed April 29, 2019).

Eory, V., Pellerin, S., Carmona Garcia, G., Lehtonen, H., Licite, I., Mattila, H., et al. (2018). Marginal abatement cost curves for agricultural climate policy: state-of-the art, lessons learnt and future potential. *J. Clean. Prod.* 182, 705–716. doi:10.1016/j.jclepro.2018.01.252

Fischer, D., Kaufmann, F., Hollinger, R., and Voglstätter, C. (2018a). Real live demonstration of MPC for a power-to-gas plant. *Appl. Energy.* 228, 833–842. doi:10.1016/j.apenergy.2018.06.144

Fischer, D., Kaufmann, F., Selinger-Lutz, O., and Voglstätter, C. (2018b). Power-to-gas in a smart city context-influence of network restrictions and possible solutions using on-site storage and model predictive controls. *Int. J. Hydrogen Energy.* 43, 9483–9494. doi:10.1016/j.ijhydene.2018.04.034

Frank, E., Gorre, J., Ruoss, F., and Friedl, M. J. (2018). Calculation and analysis of efficiencies and annual performances of power-to-gas systems. *Appl. Energy.* 218, 217–231. doi:10.1016/j.apenergy.2018.02.105

García, J. L., De La Plaza, S., Navas, L. M., Benavente, R. M., and Luna, L. (1998). Evaluation of the feasibility of alternative energy sources for greenhouse heating. *J. Agric. Eng. Res.* 69, 107–114. doi:10.1006/jaer.1997.0228

GEAB, Vattenfall, ABB, and KTH (2011). Smart grid Gotland. Repot No.: 2011-21.

Grueger, F., Möhrke, F., Robinius, M., and Stolten, D. (2017). Early power to gas applications: reducing wind farm forecast errors and providing secondary control reserve. *Appl. Energy.* 192, 551–562. doi:10.1016/j.apenergy.2016.06.131

Grüger, F., Dylewski, L., Robinius, M., and Stolten, D. (2018). Carsharing with fuel cell vehicles: sizing hydrogen refueling stations based on refueling behavior. *Appl. Energy.* 228, 1540–1549. doi:10.1016/j.apenergy.2018.07.014

Grüger, F., Hoch, O., Hartmann, J., Robinius, M., and Stolten, D. (2019). Optimized electrolyzer operation: employing forecasts of wind energy availability, hydrogen demand, and electricity prices. *Int. J. Hydrogen Energy.* 44, 4387–4397. doi:10.1016/j.ijhydene.2018.07.165

Guelpa, E., and Verda, V. (2019). Thermal energy storage in district heating and cooling systems: a review. *Appl. Energy.* 252, 113474. doi:10.1016/j.apenergy.2019.113474

Hanley, E. S., Deane, J. P., and Gallachóir, B. P. Ó. (2018). The role of hydrogen in low carbon energy futures–a review of existing perspectives. *Renew. Sustain. Energy Rev.* 82, 3027–3045. doi:10.1016/j.rser.2017.10.034

IVL (2012). Petrol costs in 2030. Available at: https://www.ivl.se/toppmeny/pressrum/nyheter/nyheter—arkiv/2012-10-18-sa-mycket-kostar-bensinen-ar-2030.html (Accessed June 5, 2020).

Janke, L., McDonagh, S., Weinrich, S., Murphy, J., Nilsson, D., Hansson, P-A., et al. (2020). Optimizing power-to-H_2 participation in the Nord Pool electricity market: effects of different bidding strategies on plant operation. *Renew. Energy.* 156, 820–836. doi:10.1016/j.renene.2020.04.080

Koohi-Fayegh, S., and Rosen, M. A. (2020). A review of energy storage types, applications and recent developments. *J. Energy Storage.* 27, 101047. doi:10.1016/j.est.2019.101047

Lagnelöv, O., Larsson, G., Nilsson, D., Larsolle, A., and Hansson, P. (2020). Performance comparison of charging systems for autonomous electric field tractors using dynamic simulation. *Biosyst. Eng.* 194, 121–137. doi:10.1016/j.biosystemseng.2020.03.017

Linde (2017a). Pure Water Knowledge: gases and application technologies for water treatment. Available at: http://www.linde-gas.com/watertreatment

Linde (2017b). Taking Oxygenation to a new level: innovative aquaculture solutions. Available at: http://www.linde-gas.lv/.

Lundblad, M. (2015). Land use on organic soils in Sweden. Report No.: 199 2015.

Mariani, L., Cola, G., Bulgari, R., Ferrante, A., and Martinetti, L. (2016). Space and time variability of heating requirements for greenhouse tomato production in the Euro-Mediterranean area. *Sci. Total Environ.* 562, 834–844. doi:10.1016/j.scitotenv.2016.04.057

McDonagh, S., O'Shea, R., Wall, D. M., Deane, J. P., and Murphy, J. D. (2018). Modelling of a power-to-gas system to predict the levelised cost of energy of an advanced renewable gaseous transport fuel. *Appl. Energy.* 215, 444–456. doi:10.1016/j.apenergy.2018.02.019

McDonagh, S., Deane, P., Rajendran, K., and Murphy, J. D. (2019). Are electrofuels a sustainable transport fuel? Analysis of the effect of controls on carbon, curtailment, and cost of hydrogen. *Appl. Energy.* 247, 716–730. doi:10.1016/j.apenergy.2019.04.060

McDonagh, S., Wall, D. M., Deane, P., and Murphy, J. D. (2019). The effect of electricity markets, and renewable electricity penetration, on the levelised cost of energy of an advanced electro-fuel system incorporating carbon capture and utilisation. *Renew. Energy.* 131, 364–371. doi:10.1016/j.renene.2018.07.058

McDonagh, S., Ahmed, S., Desmond, C., and Murphy, J. D. (2020). Hydrogen from offshore wind: investor perspective on the profitability of a hybrid system including for curtailment. *Appl. Energy.* 265, 114732. doi:10.1016/j.apenergy.2020.114732

McGreevy, R. (2013). Midlands landowners offered €18,000 a year per wind turbine. *Ir. Times.* 1. , 2013 Available at: https://www.irishtimes.com/news/midlands-landowners-offered-18-000-a-year-per-wind-turbine-1.1320270 (Accessed March 15, 2020).

McKinsey and Company (2009). *Pathways to a low-carbon economy: version 2 of the global greenhouse abatement cost curve.*New York, USA: . McKinsey and Company.

Mohseni, F., Görling, M., Llindén, M., and Larsson, M. (2017). *Genomförbarhetsstudie för power to gas på Gotland.* Stockholm: SWECO, 378.

Moradi, R., and Groth, K. M. (2019). Hydrogen storage and delivery: review of the state of the art technologies and risk and reliability analysis. *Int. J. Hydrogen Energy.* 44, 12254–12269. doi:10.1016/j.ijhydene.2019.03.041

Moreda, G. P., Muñoz-García, M. A., and Barreiro, P. (2016). High voltage electrification of tractor and agricultural machinery-a review. *Energy Convers. Manag.* 115, 117–131. doi:10.1016/j.enconman.2016.02.018

NHA (2012). New Holland's NH_2 fuel cell powered tractor to enter service. *Fuel Cell. Bull.* 2012, 3–4. doi:10.1016/s1464-2859(12)70004-4

Nilsson, D., and Hansson, P-A. (2001). Influence of various machinery combinations, fuel proportions and storage capacities on costs for co-handling of straw and reed canary grass to district heating plants. *Biomass Bioenergy.* 20, 247–260. doi:10.1016/S0961-9534(00)00077-5

NordPool (2019). *Historical market data.* Lysaker (Norway). Available at: https://www.nordpoolgroup.com/historical-market-data/ (Accessed November 15, 2019).

Novo, A. V., Bayon, J. R., Castro-Fresno, D., and Rodriguez-Hernandez, J. (2010). Review of seasonal heat storage in large basins: water tanks and gravel-water pits. *Appl. Energy.* 87, 390–397. doi:10.1016/j.apenergy.2009.06.033

Paulsson, R., Djodjic, F., Ross, C., and Hjerpe, K. (2015). Nationell jordartskartering-Matjordens egenskaper i åkermarken. Report No.: 2015:19.

Proost, J. (2019). State-of-the art CAPEX data for water electrolysers, and their impact on renewable hydrogen price settings. *Int. J. Hydrogen Energy.* 4, 4406–4413. doi:10.1016/j.ijhydene.2018.07.164

Proton Ventures B. V. (2018). Sustainable ammonia for food and power. *Nitrogen.* 1–10. Available at: https://www.protonventures.com/

wp-content/uploads/2018/09/NS-354-Small-scale-plant-design-PROTON-VENTURES-3-1.pdf (Accessed April 1, 2020).

Roda, V., Carroquino, J., Valiño, L., Lozano, A., and Barreras, F. (2018). Remodeling of a commercial plug-in battery electric vehicle to a hybrid configuration with a PEM fuel cell. *Int. J. Hydrogen Energy.* 43, 16959–16970. doi:10.1016/j.ijhydene.2017.12.171

Safa, M., Samarasinghe, S., and Mohssen, M. (2010). Determination of fuel consumption and indirect factors affecting it in wheat production in Canterbury, New Zealand. *Energy.* 35, 5400–5405. doi:10.1016/j.energy.2010.07.015

Schmidt, O., Gambhir, A., Staffell, I., Hawkes, A., Nelson, J., and Few, S. (2017). Future cost and performance of water electrolysis: an expert elicitation study. *Int. J. Hydrogen Energy.* 42, 30470–30492. doi:10.1016/j.ijhydene.2017.10.045

Skatteverket (2020). Tax refund on electrticity and fuel. Available at: https://www.skatteverket.se/foretagochorganisationer/skatter/punktskatter/energiskatter/aterbetalningavskattpaelochbransle.4.109dcbe71721adafd252816.html.

SMHI (2017). Historical wind speed measurements at Visby Flygplats. Available at: https://www.smhi.se/en (Accessed October 10, 2019).

SMHI (2020). Metereological observations at Visby Flygplats 2020. Available at: https://www.smhi.se/data/meteorologi/ladda-ner-meteorologiska-observationer/#param=precipitation24HourSum.

Stadkraft (2020). Wind parks in Sweden. Available at: https://www.statkraft.se/energikallor/kraftverk/sverige/bjorkhojden-wind-farm/ (Accessed March 15, 2020).

Thornton, G. (2019). *Renewable energy discount rate survey result–2018.* Available at: https://doi.org/https://www.grantthornton.co.uk/en/insights/renewable-energy-discount-rate-survey-2018/ (Accessed November 15, 2019).

Törnfet, A., and Nypelius, A. (2020). *Vätgas och energilagring.* Romakloster (Sweden). Available at: https://www.lrf.se/mitt-lrf/regioner/gotland/aktuellt-arbete/projekt1/ (Accessed June 1, 2020).

Ulleberg, Ø., and Hancke, R. (2020). Techno-economic calculations of small-scale hydrogen supply systems for zero emission transport in Norway. *Int. J. Hydrogen Energy.* 45, 1201–1211. doi:10.1016/j.ijhydene.2019.05.170

Vestas (2019). Specifications of wind turbine Vestas V90 2MW. Available at: https://en.wind-turbine-models.com/turbines/1681-hummer-h25.0-200kw (Accessed January 5, 2020).

Voelklein, M. A., Rusmanis, D., and Murphy, J. D. (2019). Biological methanation: strategies for in-situ and ex-situ upgrading in anaerobic digestion. *Appl. Energy*. 235, 1061–1071. doi:10.1016/j.apenergy.2018.11.006

Wallnerström, C. J., and Bertling Tjernberg, L. (2018). "11 -analysis of the future power systems's ability to enable sustainable energy—using the case system of Smart Grid Gotland," in *Application of small grid technologies*. Editors L. A. Lamont and A. Sayigh (Stockholm: Academic Press), 373–393.

Wiederholm, J., Castegren, G., Ulaner, M., Persson, M.-L., and Lindbäck, M. (2018). *Nils Holgerssons underbara resa genom Sverige.* Stockholm: Nils Holgerssongruppen.

Witney, B. (1988). *Choosing and using farm machines.* Madison, WI: Longman Scientific and Technology.

Woynarovich, A., Hoitsy, G., and Moth-Poulsen, T. (2011). *Small-scale rainbow trout farming.* Rome: FAO.

Wu, D., Ren, J., Davies, H., Shang, J., and Haas, O. (2019). Intelligent hydrogen fuel cell range extender for battery electric vehicles. *World Electr. Veh. J.* 10, 181573753. doi:10.3390/wevj10020029

Yan, M., Cheng, K., Luo, T., Yan, Y., Pan, G., and Rees, R. M. (2015). Carbon footprint of grain crop production in China - based on farm survey data. *J. Clean. Prod.* 104, 130–138. doi:10.1016/j.jclepro.2015.05.058

Zauner, A., Böhm, H., Rosenfeld, D. C., and Tichler, R. (2019). Analysis on future technology options and on techno-economic optimization. Report No.: D7.7.

Conflict of Interest: The authors declare that the research was conducted in the absence of any commercial or financial relationships that could be construed as a potential conflict of interest.

GLOSSARY

List of abbreviations

CAPEX capital expenditures

CCU carbon capture and utilization

CH_4 methane

CO_2 carbon dioxide

FCAM fuel cell agricultural machinery

FCMV fuel cell minivan

GHG greenhouse gas

H_2 hydrogen

H_2O water

KOH Potassium hydroxide

$LCOH_2$ levelized cost of hydrogen

NCF net cash flow

NH_3 Ammonia

NOH non-operating hours

NPV net present value

O_2 oxygen

OPEX operational expenditures

PEM proton-exchange membrane

PSA pressure swing adsorption

PtH_2 power-to-hydrogen

$PtCH_4$ power-to-methane

PtX power-to-X

TRL technology readiness levels

VRE variable renewable electricity

WH waste heat

List of model parameters and symbols

b percentage of solar radiation contributing to sensible heat (decimal)

C_{cold} electricity costs to keep the electrolyser on cold standby (€)

$C_{comp,i}$ electricity costs with H_2 compression (€)

$C_{elec,i}$ electricity costs during the electrolyser operation (€)

C_{total} total electricity costs (€)

E_i electrolyser operation mode (binary)

f_{heat} fraction of power consumption that becomes available heat (decimal)

H hourly demand for heat per greenhouse ground area (W/m^2)

i index (hour i)

$m_{H_2,i}$ H_2 production in each hour i (kg)

$m_{H_2O,i}$ H_2O consumption in each hour i (kg)

$m_{O_2,i}$ O_2 production in each hour i (kg)

ρ_{H2} H_2 density (g/L at STP)

P_N electrolyser's nominal rated power (MW)

R_{ON} run hours of the system per year

r_{H_2} molar ratio of H_2/H_2O

r_{O_2} molar ratio of O_2/H_2O

S global solar radiation (W/m^2)

τ transmissivity of the cover (-);

T_{air} outdoor air temperature (°C)

T_{grid} electricity grid tariff (€/MWh)

T_{in} temperature in the greenhouse (°C)

$T_{spot,i}$ electricity price in the day ahead spot market (€/MWh)

U average heat transfer coefficient per ground area (W/m^2K)

$V_{H_2,i}$ gas storage volume in each hour i (m^3 H_2 at 500 bar)

$V_{H_2,max}$ available gas storage size (m^3 H_2 at 500 bar)

$W_{cold,i}$ power consumption during cold standby (kWh)

W_{comp} H_2 compressor's specific power consumption (kWh/kg H_2)

W_{elec} hourly power consumption of the electrolyser on full load (kWh)

$W_{H_2,i}$ specific power consumption during operation (kWh/m^3 H_2 at STP)

W_{safe} power consumption for safety infrastructure (kWh)

$W_{total,i}$ total power consumption during H_2 production (kWh/kg H_2)

$W_{wind,i}$ wind power production in each hour i (MWh)

$W_{heat,i}$ waste heat production in each hour i (kWh)

APPENDIX A. GREENHOUSE HEAT DEMAND

The produced waste heat was assumed to be used in a nearby greenhouse for tomato production. A simplified model was used to calculate the hourly demand for heat (H) per greenhouse ground area according to the method described below (García et al., 1998):

$$H = U\,(T_{in} - T_{air}) - b\tau S \tag{A1}$$

where U is the average heat transfer coefficient per ground area (W/m^2K); T_{in} is the temperature in the greenhouse (°C); T_{air} *is* the outdoor air temperature (°C); b *is* the percentage of solar radiation contributing to sensible heat (decimal); τ *is* transmissivity of the cover (-); S is the global solar radiation (W/m^2).

For appropriate growing conditions, the temperature in the greenhouse (T_{in}) was assumed to be 22°C during daytime (i.e. when $S > 0$) and 15°C during nighttime (i.e., when $S = 0$). The values of U, b and τ were assumed to be 5.0 W/m^2K (Mariani et al., 2016), 0.4 (García et al., 1998) and 0.7 (Mariani et al., 2016), respectively. The hourly values of T_{air} and S were obtained from two metereological stations near the city of Visby (Gotland, Sweden), located at 57°39′N 18°20′O and 57°40′N 18°20′O, respectively. In the described model, $H = 0$ when $T_{air} \geq T_{in}$ *or* $b\tau S \geq U\,(T_{in} - T_{air})$.

Based on weather data for the year 2019, it was observed a significant demand for heat in winter, spring, and autumn. Also, heat demand was observed in summer, however mostly during night time. Considering data between 1961 and 1990, the summertime in 2019 was around 2.0°C warmer than average values on Gotland, and the average temperature during 2019 was on average 2.1°C warmer than what could be considered as normal.

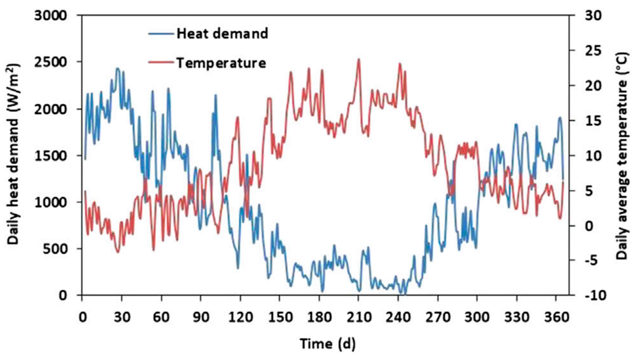

FIGURE A1 | Simulated daily heat demand in a greenhouse for the production of tomatoes and the daily average air temperature on Gotland, Sweden.

APPENDIX B. OPTIMAZATION OF ALL CASES ASSESSED

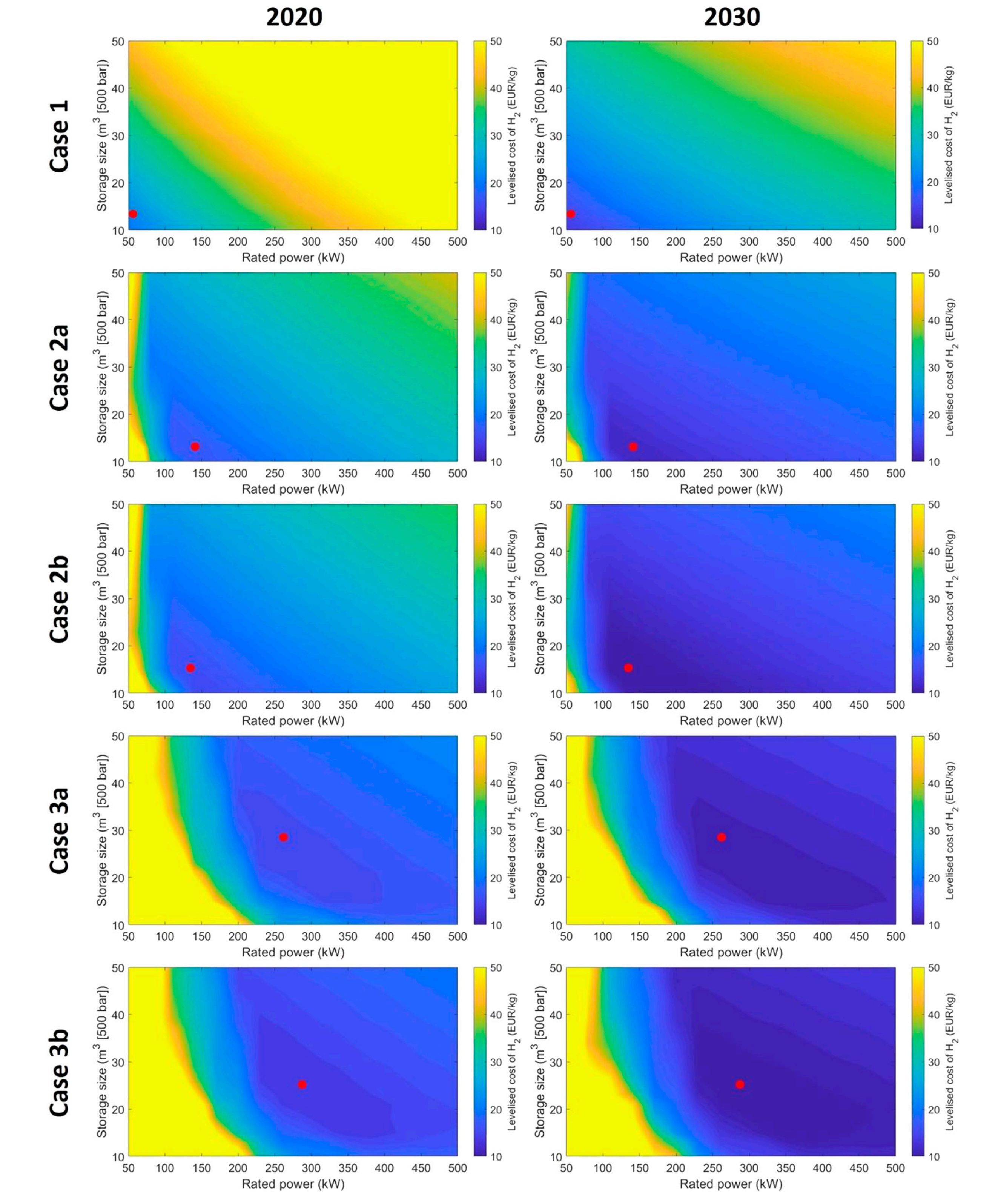

FIGURE A2 | Optimization of PtH_2 plant configuration ($LCOH_2$). Note: Red dot shows the optimal plant configuration to minimize $LCOH_2$.